A Comprehensive Review on Design aspects and Performance Characteristics of Solar Parabolic Trough Collector

Himanshu R. Patel*ᵃ ID , Vikram B. Patel** ᵃ ID , Anil R. Chaudhari***ᵇ ID

* ᵃPh.D. Scholar, Faculty of Science and Technology, Mechanical Engineering, Ganpat University, Kherva, Mehsana, Gujarat, India

**ᵃ Professor, Mechanical Engineering, Research Guide Ganpat University, L. E. College, Morbi, Gujarat, India

*** ᵇAssistant Professor, Dairy Engineering Department, MIDFT, Mehsana, Gujarat, India

(himanshu@midft.com , avivikram@yahoo.com, anil@midft.com)

‡ Himanshu R. Patel; Vikram B. Patel, Ganpat University, Kherva, Mehsana, Gujarat, India, Tel: +91 9712433209,

,himanshu@midft.com

Abstract- Parabolic trough collector is being widely used for harnessing the abundantly available solar energy for thermal and electrical applications. Parabolic trough collector system concentrates solar radiation using a parabolic trough/curved shaped mirror throughout the line of focus where heat absorber tube is placed from which heat transfer fluid is circulated and temperature of Heat Transfer Fluid be increased. Parabolic trough collector's essential geometrical dimensions are discussed for estimating size and material requirement for initial design and fabrication phase. Present review paper also includes structure of collector,reflector,receiver, Heat transfer fluid, Sun tracking system and Thermal enrgy storage. This review paper incorporates researchers work on thermal efficiency enhancement using base thermic fluids like water,synthetic oils, molten salts,mineral oil etc and benefits of addition of nanoparticles (Copper,Copper oxide, Aluminium oxide, Graphene oxide, SWNCT-single wall carbon nano tubes, MWCNT-multi wall carbon nanotubes and Sic-silicon carbide etc) with base fluid. Therefore selecting right design to develop such collector with highest achievable performance with fewer or zero complication, it is important to study all the components in details. The performance factors (Geometrical, optical and thermal), design modifications, component alterations by brief study of different researchers and attempts to illustrate crucial parameters that drive performance efficiency of PTC system are discussed thoroughly in this review. The paper reveals that Solar Parabolic Trough collector is the most promising concentrated solar power technology for satisfying medium and large scale industrial thermal energy requirement.

Keywords Parabolic Trough Collector; receiver, geometrical dimensions, optical and thermal parameters, Sun tracking system, thermic fluids.

1. Introduction

There are two ways for harnessing the freely and abundant green energy from the Sun, first one is solar thermal and second one; the younger than prior is Photo-Voltaic. Although electricity generation from PV system is environment friendly, they have low conversion efficiency, low energy potential and high investment costs. Solar PV system is widely applicable to heating, lighting, irrigation, off grid and on grid[1]–[4]. The various ways to harvest solar thermal energy includes box type solar cooker, Flat Plate Collector (FPC), Evacuated Tube Collector (ETC), Concentrated Solar Power (CSP), tower system etc. Concentrating solar rays/energy can be achieved through different devices such as Scheffler Reflector, Longitudinal Fresnel Collector (LFC), Solar Tower System, Paraboloid Dish Concentrator, Parabolic Trough Collectors (PTC) and Compound Parabolic Collectors (CPC).

Kalogirou 2004 reported that Sun total energy output is 3.8 X 10^{20} MW and the earth receives a minuscule fraction that is 1.7 X 10^{14} kW, on the other hand this small fraction, falling for one and half hour on the earth is equivalent to the global annual energy demand which is about 900 X 10^{18} Joule[5]. India, being a tropical country has an advantage of Sun energy that can be used for a variety of applications. The daily average solar insolation over India is in the range 4 to 7 kWh per square meter area [6].

PTCs systems are in use because of its easy to scale-up, versatility, high power capacity, modularity, high productivity, longer service life and compatibility with major heat transfer fluids (HTF). PTCs can achieve 400 °C with the use of thermal oils, applicable to produce electricity [7], [8].

2. Design considerations of basic components of PTC

Most elementary PTC system consists of solar reflector/concentrator with energy receiver which is mounted over a support structure. A heat transfer fluid (HTF) receives the solar energy in the absorber and transfers heat tothe secondary system. A sun tracking mechanism is used for maintaing the consistant output from the system. The constructional and design aspects of the PTC are decided by applicability of the system and consequently addition or subtraction of any component into the system depends on final requirements e.g. energy storage component.

2.1. Structure of Parabolic Trough Collector

Collectors have been defined according to various dimensions as width of aperture, focus distance, length of trough and rim angle and it plays important role in PTC system, so researchers are continuously optimizing its geometrical parameters. Figure 1 depicts relation amongst the dimensions viz. focal length, rim angle and aperture width. Variation in any such geometrical dimensions directly alters the dimensions of other one. For example, to increase focal length, the aperture width will be increase. Higher value of rim angle enlarges parabolic radius but simultaneously lower down the focal length and aperture area.
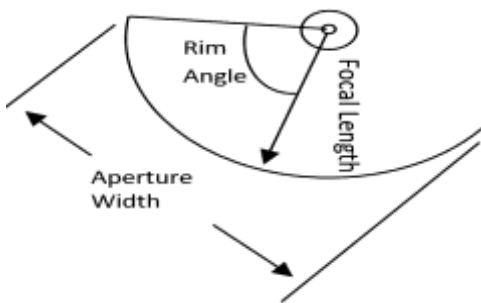

Figure 1. Illustration of Rim angle, focal length and aperture width.

In 2014, Schweitzer and co-workers developed largest collector till date with the dimensions of 247m length and aperture width of 7.5m[9]. In the same year 2014,

Montes et. al designed and created a Solar Parabolic Trough Collector (SPTC) using innovative modern manufacturing processes and material selection with aim of quicker installation with cost effective production [10]. Some of the features included as new traction wheel-based tracking system, which consume low power and had high precision; all these things weighed only 50 kg, which makes it very suitable for transportation. For 1 litre of water, it takes 2 seconds only to reach 80 ºC and that result into 60% thermal efficiency. Arasu and Sornakumar designed fibreglass reinforced PTC in 2007,considering the weather condition of Madurai city of India, which can withstand up to 72 kg wind force without affecting reflectance of trough i.e. 0.974 [11].

A novel model developed and compared by Behar et al., 2015, with Engineering Equation Solver (EES) resulted more accurate in thermal performance [12]. Researcher also summarized by relating the results of previous studies approved in the utmost calibrated laboratories globally. Zou et al. 2017, calculated the output of PTC when there is no incident angles, besides that studied the results of geometrical terms (aperture width, focal distance, size of absorber tube, size of glass tube, the rim angle and radial angle of the Sun) on optical performance. A Monte Carlo Ray Tracing (MCRT) technique was applied by team to evaluate SEGS LS-2 PTC Unit. The summary of this research is that increasing aperture width helps in surge of local concentration [13].

Upadhyay et al. (2017) offered flexible, easy to assemble and compact PTC design without drop in its compatibility. Many objective for such design is to test diverse parameters like aperture length-width, several HTFs, various material of receiver and reflective materials [14]. Paetzold et al. (2014) worked on studying the consequences of wind on performance of PTC in which it was derived using CFD programme that the effects of bigger wind stress on the PTC were largely noticed at pitch angles between 15° and 60° [15]. MicroSolar named proto-type PTC power plant was experimented by Agagna et al. (2018) for thermal and optical performance. Figure 2 shows photograph of three PTC set- ups, one is facing North-south, and two others are facing east-west[16].

Figure 2. MicroSol-R [16]

2.1.1 Parabolic geometrical dimensions

A parabolic trough is the chief component of the Solar parabolic trough collector system. SPTC's fundamental geometrical dimensions are focal distance, rim angle,

aperture width, size of the absorber/receiver, concentration ratio, trough length, aperture area and parabola arc length etc.

If the starting point is drawn at the vertex 'v' then the equation of the parabola is, in terms of the x-y coordinate system is given as, equation (1) [17]. Equation 1 represents parabola.

$$f = \frac{x^2}{4y} \tag{1}$$

where f is termed as focal length.

Figure 3 shows the physical dimensions of parabolic trough geometry which are focal distance (f), rim angle (ϕ_{rim}), aperture width (w_a), size of receiver/ absorber(D_o) and trough length (L).
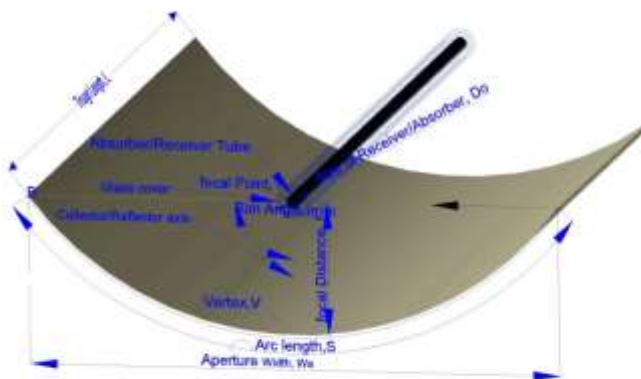

Figure 3. Basic geometrical terminologies of SPTC

Focal distance (f). The focal distance may be defined as the vertical dimension drawn from the vertex of the parabola to the focal Point, this could be imagined when parabola is facing solar noon as shown in Fig.3 and is given by equation (2) [17]–[19].

$$f = \frac{w_a}{4 \tan\frac{\phi_{rim}}{2}} \tag{2}$$

where, W_a= width of aperture and ϕ_{rim}= rim angle

Rim Angle (ϕ_{rim}). The another important characteristics i.e. rim angle is defined as the angle included by the line joining the focal point to the mirror reflector and the optical axis. It may be described by VFB as shown in Fig.3 and given by equations (3) and (4) [20], [21].

$$\phi_{rim} = \sin^{-1}\frac{w_a}{2r_r} \tag{3}$$

or

$$\phi_{rim} = \tan^{-1}\left[\frac{8 \cdot \left(\frac{f}{w_a}\right)}{16 \cdot \left(\frac{f}{w_a}\right)^2 - 1}\right] \tag{4}$$

The ratio of focal distance and width of aperture would be given by equation (5) [22], [23].

$$\frac{f}{w_a} = \frac{1 + \cos\phi_{rim}}{4 \sin\phi_{rim}} \tag{5}$$

The beam radiation incident at point 'B' on the mirror reflector where radius is maximum at r_r as shown in Fig.3 and would be given as equation (6) [19], [24].

$$r_r = \frac{2 \cdot f}{1 + \cos\phi_{rim}} \tag{6}$$

Aperture width (w_a). The aperture width is defined as the distance between free edges of parabolic trough Fig.3 which also describe the entrance of the parabola.

The relation between aperture width with rim Angle (ϕ_{rim}) may be given by the equations (7), (8) and (9) [18].

$$w_a = 2 \cdot r_r \cdot \sin\phi_{rim} \tag{7}$$

or

$$w_a = \frac{4 \cdot f \cdot \sin\phi_{rim}}{1 + \cos\phi_{rim}} \tag{8}$$

which reduce to

$$w_a = 4 \cdot f \cdot \tan\frac{\phi_{rim}}{2} \tag{9}$$

Size of the receiver/absorber (D_o). For a mirror like reflection of solar radiation by parabolic collector of perfect profile and alignment, the diameter of the absorber to capture all of the incident solar radiation is shown by Fig.3 and can be given by equations (10) and (11) [17], [25].

$$D_o = 2 \cdot r_r \cdot \sin 0.267 \tag{10}$$

or

$$D_o = \frac{w_a \cdot \sin 0.267}{\sin\phi_{rim}} \tag{11}$$

Trough length (L). Trough length (L) is described as the longitudinal distance in z direction as shown in Fig.3.

Parabola height (h_p). The equation of parabola height (h_p) is given by equation (12) [21], [23].

$$h_p = \frac{w_a^2}{16 \cdot f} \tag{12}$$

Arc length of reflective mirror (S). An arc length (S), as an additional dimension can be useful in understanding solar collector design as given in equation (13) [19], [24].

$$S = \frac{h_p}{2}\left\{\sec\frac{\phi_{rim}}{2} \cdot \tan\frac{\phi_{rim}}{2} + \ln\left[\sec\frac{\phi_{rim}}{2} \cdot \tan\frac{\phi_{rim}}{2}\right]\right\} \tag{13}$$

Geometrical Concentration ratio (C_G). For a tubular absorber, the concentration ratio 'C_g' is described by the ratio of reflector aperture area (A_a) to the absorber surface area and given by the equation (14) [20], [26].

$$C_G = \frac{w_a \times L}{\pi \cdot D_0 \times L} = \frac{w_a}{\pi \cdot D_0} \qquad (14)$$

Aperture Area (A_a). The aperture area describe the Sun's energy collection at a given DNI and at a given Sun location. The aperture area also express essential constructive measure.

It can be defined as the multiplication of aperture width (w_a) with the trough length (L) in m^2 and is given by equation (15) [24], [27].
Mathematically,

$$A_a = W_a \cdot L \qquad (15)$$

The surface area (A) of parabolic cavity could be of important for estimation of reflective material requirement and given by equation (16) [27].

$$A = \left[\frac{w_a}{2} \cdot \sqrt{1 + \frac{w_a^2}{16 \cdot f^2}} + 2f \, \ln\left(\frac{w_a}{4 \cdot f} + \frac{w_a^2}{16 \cdot f^2} \right) \right] \cdot L \quad (16)$$

The effective aperture area may be calculated by equation (17) [24].

$$A_a = (W_a - D_o) \cdot L \qquad (17)$$

where, D_o = outer diameter of absorber in meter

Table 1 shows parabolic trough collectors and receivers significant Geometrical dimensions used by researchers in previous investigations.

3. Reflector

Curved glass mirror with silver coating is commonly used as reflector and that is the most vital and expensive component of PTC system. Higher the reflectivity of reflector makes it more costlier. To minimize the cost of PTC system few alternatives are also under development and are in the applications also, i.e. aluminium foil, anodised aluminium sheets, silver coated PVC sheets etc.

Sagade, Aher, and Shinde (2013) worked on fibreglass reinforced plastic coated with aluminium foil as trough and achived reflectivity of 0.86. Reflectors made of black proxy material and coated mild steel resulted into 51 % efficiency and 39% efficiency with and without glass cover respectively [28]. Sagade, Shinde, and Patil (2014) achived 81.70°C by using 10 micron thick aluminium foil as reflector and copper absorber [29]. Arasu and Sornakumar (2007) developed FRP parabolic trough collector with SLARFLEX foil having smooth 90° rim angle and 0.974 reflectance.

The significant optical parameters like reflectivity of mirror, absorptivity of receiver and transmissivity of glass cover etc. in conjunction with weather data used by researchers in previous investigations are as shown in Table 2.

4. Thermic Fluids and Nanoparticles

Solar heat is required to be transferred from receiver to end use, thermic fluids are greatest medium and widely being used in PTC. Synthetic oils, water or molten salt has been commonly used to enhance the efficiency and transferring of heat. Nanofluid particles have been applicable efficiently by researcher worldwide. Figure 4 shows schematic representation of molten salt based thermic fluid system used in solar tower system, cold salt at 290°C is circulated in system and heated upto 565°C in receiver by sun reflected rays from heliostat [30].
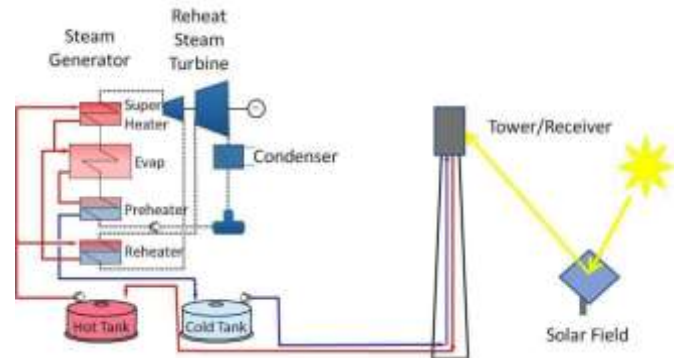

Figure 4. Schematic flow diagram of Molten Salt as Thermic fluid [30]

Evangelos Bellos (2019) did investigations on the six different nanoparticles (Copper-Cu, Copper oxide-CuO, Ferric oxide-Fe$_2$O$_3$), Titanium dioxide-TiO$_2$, Aluminium oxide-Al$_2$O$_3$ and Silicon dioxide-SiO$_2$) added with oil, and suggested that 6% Copper-Cu solution gives maximum thermal efficiency of 74% [31]. A vast range of material reviewed by Hussein on Silicon Dioxide-SiO$_2$ and Water-H$_2$O, Aluminium Oxide--Al$_2$O$_3$ or synthetic oil, MWCNT-Multi-walled carbon nanotubes or mineral oil, and gas based nanofluids. MWCNT/mineral oil solution can enhance efficiency up to 5% compared to pure oil as Thermic fluid [32]. Zaversky et al. 2013 studied molten salt as heat transfer fluid and achieved maximum 520°C [33].

Ghasemi and Ranjbar (2016) added Al$_2$O$_3$ into water and achieved 28% increase in heat transfer, all this be simulated mathematically for forced convection heat transfer, eddy current flow is used with nanofluid in the PTC receiver. Furthermore, addition of 3% nanoparticles of CuO to water resulted in 35% improvement in heat transfer [34]. Tzivanidis and Antonopoulos (2016) observed 42%, 42.21%, and 40.12% efficiency of CO$_2$, Helium and Air respectively, whereas Liquid sodium exhibit 47.48% efficiency as Thermic fluid [35].

Table 3 reveals significant effect of HTF's (Water, steam, pressurized water, Therminol vp-1, syltherm-800, solar salt, liquid sodium, air, super critical CO$_2$, dowtherm-A and shell thermia oil B etc.) on thermal performance of PTC. Also use of various nanoparticles (CU,CUO,Al$_2$O$_3$, Graphene oxide, SWNCT-single wall carbon nano tubes, MWCNT-multi wall carbon nanotubes and Sic-silicon carbide etc.) upto 5% concentration with base HTF's explain the enhanced outlet fluid temperature together with thermal efficiency improvement.

Table 1. Summary of Geometrical dimensions used in previous investigations

Ref	Collector/Reflector Geometrical dimensions								A_a	C_G
	f	ϕ_{rim}	W_a	L	Absorber Diameter		Glass cover Diameter			
					D_o	D_i	D_{co}	D_{ci}		
	(m)	(°)	(m)	(m)	(m)	(m)	(m)	(m)	(m²)	
Praveen and Chandra 2022[36]	2.11	-	5.75	8.33	0.07	0.066	0.125	0.1196	47.89	-
K. Zhao et al. 2022[37]	-	-	5.76	4.08	0.07	0.066	0.115	0.109	23.5	68.7
Ghodbane et al. 2022[38]	1.84 1.88	30, 70, 90	5	7.8	0.07	0.066	0.120	0.115	39	19.1 22.54
Shaker et al. 2022[39]	1.84	-	5	7.8	0.07	0.066	0.115	0.109	39	22.74
Mohammadi et al. 2021[40]	-	-	-	-	0.08	0.076	0.120	0.115	656	-
Khan et al. 2021[41]	-	-	-	3.125	0.056	0.052	0.097	0.067	-	-
A. Mohammad et al. 2021[42]	-	-	1.2	3	0.0311	0.02875	0.04826	0.0537	3.6	-
Pal and K 2021[43]	-	80	5.76	12	0.07	0.05	0.125	0.122	-	-
Nascimento, Zavaleta-aguilar, and Sim 2021[44]	-	-	3.5	7.34 5.82 1.22 7.85	0.05	0.04	0.090	-	-	-
Alnaqi, Alsarraf, and Al-rashed 2021[45]	-	-	-	3.6	0.054	0.05	0.069	0.065	-	-
Malekpour, Ahmadi, and Sadeghzadeh 2021[46]	-	-	1.2	3	0.0311	0.02875	0.048	0.0537	3.6	-
Nguimdo, Teka, and Fopossie 2021[47]	-	-	47	5	0.07	0.066	0.115	0.109	-	-
S. Mohammad, Hosseini, and Sha 2021[48]	0.3	90	1.2	1.5	0.037	-	0.470	-	1.8	-
Bellos, Tzivanidis, and Said 2020[49]	1.84	-	5	7.8	0.07	0.066	0.115	0.109	39	22.7
Fathabadi 2020[50]	-	-	0.3	0.24	-	-	-	-	0.72	7.5
Reddy and Ananthsornaraj 2020[51]	1.71	80.3	5.77	4.06	0.07	0.066	0.125	0.119	23.42	26.3
Z. Zhao et al. 2020[52]	0.7	83.5	2.5	8	0.04	0.036	-	-	20	19.9
Thappa et al. 2020 [53]	-	14 80	5.76 5.76	12.27 12.27	0.07 0.016	0.065 0.011	0.109 0.115	0.027 0.024	70.67 70.67	15.95 67.9
Subramani, Sevvel, and Srinivasan 2020 [54]	0.024	80	0.8	2	0.016	0.013	0.034	0.03	1.6	-
Malan and K 2020[55]	-	80	5.77 9	4	0.07 0.110	0.066 0.106	0.120 0.160	0.116 0.156	23 36	26.23
Eduardo et al. 2020[56]	0.285	70	0.8	1.7	0.058	0.047	-	-	1.36	4.39
Abdulhamed et al. 2020[57]	0.328	90	0.1314	3	0.051	0.05	-	-	-	-
Xu et al. 2019 [58]	1.71	-	5.76	4.06	0.07	0.066	0.125	0.119	3317.8	-
Wang et al. 2019[59]	1.84	90	5	7.8	0.07	0.066	0.115	0.109	39	20
Ehyaei et al. 2019[60]	0.8	-	2.3	4.5	0.051	0.047	0.074	0.07	-	-
El Ydrissi et al. 2019[61]	2.75	-	6.47	2.61	-	-	-	-	16.886	81

Marefati, Mehrpooya, and Behshad 2018[62]	0.8	-	2.3	6.1	0.051	0.047	0.074	0.07	14	-
Hoseinzadeh et al. 2018[63]	0.175	90	0.7	2	0.026	-	0.060	-	1.4	8.5
Shawky and Khalil 2018[23]	0.6	48.06	1.2	2.5	0.0254	0.0194	-	-	3	-
Tagle-Salazar, Nigam, and Rivera-Solorio 2018[64]	0.34	-	1.1	3	0.0254	0.0194	0.044	0.04	3.3	-
Mwesigye, Yılmaz, and Meyer 2018[65]	-	80	9	5	0.080	0.076	-	0.12	45	113
Qu et al. 2017[66]	1.71	-	5.77	1.2	0.07	0.064	0.120	0.114	692	82
Sallaberry, Valenzuela, and Palacin 2017[67]	1.71	-	5.77	75	0.07	-	-	-	409.9	-
Jamal-Abad, Saedodin, and Aminy 2017[68]	0.25	90	1	1.28	28	-	-	-	1.28	-
Houcine et al. 2017[69]	1.84	90	5	7.8	0.07	-	0.115	-	39	50
Zou et al. 2017[70]	1.84	-	5	7.8	0.07	-	0.115	-	39	-
Ebrahim Ghasemi and Akbar Ranjbar 2017[71]	-	-	-	2	0.076	0.07	0.120	-	-	-
Ameen et al. 2017[72]	-	82.2	1.5	5	0.0286	-	-	-	7.5	16.7

Table 2. Summary of optical parameters and weather data used in previous investigations

Ref.	Reflectance of mirror collector	Absorptivity of receiver/absorber	Emmitance of the receiver/absorber	Emmitance of the glass cover	Transmittance of the glass cover	Weather data			Maximum Optical Efficiency	Major Outcomes
						Ambient Temperature	Solar irradiation 'DNI'	Wind speed		
						°C	W/m^2	m/s	%	
Praveen and Chandra 2022[36]	0.935	-	-	-	-	-	-	-	87	100 MW PTC CSP plant in Abha, Saudi Arabia was analyzed using fuzzy non-linear programming based optimisation approach with Genetic algorithm and concluded that proposed plant can generate an annual energy of 567.96 GWh with a plant efficiency of 17.42% and a Capacity Factor of 64.9%.
K. Zhao et al. 2022[37]	-	solel:0.960 huiyin:0.936 PTR70:0.957 TPV: 0.866	-	0.965	0.96	25	950	2	-	Temperature range of absorber coatings Solel, PTR 70, Huiyin and TPV are 20–160^{0}C, 160–350ºC, 350–480ºC, and greater than 480 ºC, respectively.
Ghodbane et al. 2022[38]	0.93	0.98 0.96 0.85	0.14	0.86	0.95	-	933.7 937.9 920.9	-	89.38	Copper receiver tube with black coating showed optical efficiency (89.38%) at focal distance 1.88 m. which was earlier estimated to be 75.77% with a focal distance of 1.84 m.
Shaker et al. 2022[39]	0.94	0.96	-	-	0.96	-	-	-	75.5	The results indicate that by changing the arrangement of the turbulators, the heat transfer efficiency of the collector can be increased by 5 % for 350K, 3.5 % for 450 K and 1% for 550 K inlet temperature.

Mohammadi et al. 2021[40]	0.93	0.963	-	-	0.964	-	750	-	84.85	The annual total pollutants can be avoided up to 3,582,422.47 kg CO_2, 147.99 kg PM, 3,341.66 kg NOx, and 14.32 kg SO_2 by designed plant.
A. Mohammad et al. 2021[42]	0.9	-	-	-	-	29-31	-	0-5	-	-
Pal and K 2021[43]	-	0.95	0.15	0.86	-	-	750	-	-	-
Nascimento, Zavaleta-aguilar, and Sim 2021[44]	0.935	0.93	-	0.87	0.89	25	1000 750 400	5	-	Authors reported that a receiver (evacuated) with absorptivity= 0.95 and emissivity= 0.1 could reduce PTC length by 84% compared to absorptivity=0.8 and emissivity=0.9.
Gharehdaghi et al. 2021[73]	-	-	-	-	-	24.4 25.8 30.6 32.2 33.3	740.3 1125.87 1286.21 1178.33 831.11	3.6 5.2 5.2 3.6 5.2	-	Exergy efficiency of the PTC which is at its maximum at 48.6% at 8 Am, decreases to 46.4% at noon and then increase to 46.6% at 4 PM.
Malekpour, Ahmadi, and Sadeghzadeh 2021[46]	0.9	-	-	-	-	16.375 19.3 6.45	720.74 776.78 761.45	0-5	-	Latent thermal energy stored in Phase change material can be used to maintain the indoor air temperature for more than 4 h after sunset.
Nguimdo, Teka, and Fopossie 2021[47]	0.94	0.94	-	-	0.95	-	-	-	75	Optical efficiency ranged between 0.73 and 0.75
Bellos, Tzivanidis, and Said 2020[49]	82.2	95	0.05 to 0.95	0.86	93.5	10 to 40	300 to 1000	0 to 10	78.4	Authors reported maximum optical efficiency is 78.4% for bare tube because no cover transmittance optical losses.

Fathabadi 2020[50]	-	93	8	-	-	-	-	-	78	The author reported power production density of the constructed solar PTC is 808.33 Wm^{-2} that is higher than ETC (710.05 Wm^{-2}) and FPC (754.86 Wm^{-2}).
Reddy and Ananthsornaraj 2020[51]	94	-	0.06-0.11	-	96	37.1	834	-	71	Authors have carried out experiment for both evacuated receiver and non evacuated receiver and obtained peak optical efficiency of 70% and 66% respectively.
Thappa et al. 2020[53]	-	0.88	0.31	0.88	-	20	-	-	-	Concentration ratio C = 67.9 achieved higher energy gains.
Malan and K 2020[55]	-	0.85	$0.062 + (2 \times 10^{-7}) \times T^2_{abs}$	0.89	-	13.95 5.6 6.37 6.13 6.38	938 985 985 991 1029	-	-	Designed a large PTSC with 9 m aperture, 110 mm absorber diameter with an intercept factor of 0.94.
Eduardo et al. 2020[56]	0.95	0.930-0.960	-	-	0.95	C_2 21.35,22.89, 19.42 C_3 20.44,21.42, 20.87	-	-	-	-	-
Xu et al. 2019[58]	-	-	-	-	-	25	900	4	-	-	-
Wang et al. 2019[59]	0.93	0.96	-	-	0.95	25	933.7 937.9, 920.9, 880.6, 909.5, 968.2, 982.3	-	-	-	-
Ehyaei et al. 2019[60]	0.94	0.9	-	0.86	0.9	30	-	-	-	-	-

Marefati, Mehrpooya, and Behshad 2018[62]	0.9	0.95	0.1	0.88	0.85	-	-	Tabriz-4.82 Tehran-3.08 Yazd-1.82 Shiraz-3.98	64.07 63.67 67.06 65.96	The average annual optical efficiencies of the PTC collector ranged between 24-37 % for Tabriz, Tehran, Yazd and Shiraz.
Hoseinzadeh et al. 2018[63]	0.76	0.98	-	-	0.9	-	-	-	65	The maximum optical efficiency were 65% for aperture width of 0.6 m with rim angle 100° and receiver diameter of 0.025 m
Shawky and Khalil 2018[23]	0.9	0.8	0.1	-	-	-	-	-	-	-
Tagle-Salazar, Nigam, and Rivera-Solorio 2018[64]	0.86	0.87	-	-	0.97	43 31.1 30.7 30.4 31.3 30.5 39.2 38.4	839 810 818 743 831.7 841.2 855.8 905.3	2	-	-
Mwesigye, Yılmaz, and Meyer 2018[65]	0.96	0.96	-	-	0.97	27	1000	2	-	-
Qu et al. 2017[66]	0.94	0.94	0.14	-	0.95	N-S tracking (June-2 31-34,Nov-5 17-19) Rotatable axis tracking (June-24 37-39, Nov-2 17-19)	June-2 638-737 Nov-5 133-614 June-24 425-693 Nov-2 208-619	June-2 0.3-4.9 Nov-5 1.6-6.2 June-24 0.3-4.2 Nov-2 0.3-4.3	-	-
Sallaberry, Valenzuela, and Palacin	0.92	0.94-0.95	-	-	0.92-0.96	-	594-1039	0.2-6.4	-	-

2017[67]										
Houcine et al. 2017[69]	0.93	0.96	-	-	0.95	-	-	-	-	Maximums solar gains reached 168.55% and 115.49% at 8 am and 4 pm, which equals to daily average gain 33.08%.
Zou et al. 2017[70]	0.93	0.96	-	-	0.95	-	-	-	-	Effect of sunshape and incident angle are investigated using Mont carlo ray tracing method for optical performance and result showed that, the optical efficiency decreases from 84.85% to 77.42%, when the circumsolar ratio (CSR) is increased from 0 to 0.5.
Ameen et al. 2017[72]	83	88	0.49	-	-	-	-	-	-	-

Table 3. Summary of base fluid, nanoparticles, HTF flow rates, inlet and oulet fluid temperature and thermal efficiency used in previous investigations

Ref.	Heat transfer fluid				Inlet fluid Temperature	Outlet fluid Temperature	Maximum Thermal Efficiency	Maximum absorber fluid Temperature	Major Outcomes
	Base fluid	Nano-particles	Nano-particles concentration	HTF flow rate					
			%	LPM	°C	°C	%	°C	
Praveen and Chandra 2022[36]	Hitec solar salt	-	-	-	293	525	-	525	Efficiency 17.42% at a Capacity Factor of 64.9%.
K. Zhao et al. 2022[37]	-	-	-	9 kg/s	-	-	-	550	The heat loss of the multi-section system was reduced by 29.3%, and the thermal efficiency was enhanced by 4.3% with an operating temperature of 290–550°C.

Ghodbane et al. 2022[38]	Syltherm-800	-	-	0.6782, 0.6208, 0.5457 kg/s	102.2 297.8 379.5	127.1 319.9 401.3	70.78 67.59 64.49	379.5	The results show that the PTC thermal effectiveness is dependent to the DNI, MFR and the thermophysical characteristics of the working fluid
Shaker et al. 2022[39]	Syltherm oil	Al_2O_3	5	4.5,6.5,8.5 kg/s	77 177 277	-	72.324	-	The increse in volume fraction of nanoparticles (5%) and number of turbulators resulted in rise in heat transfer coefficient (h) of the fluid.
A. Mohammad et al. 2021[42]	Shell thermia oil B	-	-	0.5 to 3	-	-	-	-	Results shows that the optimal selection of the rotational speed can reduce and control the temperature of the absorber fluid about 60% and surface temperature about 15%. Furthermore, about 17% enhancement in the efficiency of the PTC.
Pal and K 2021[43]	Water Steam	-	-	0.3 to 0.6 kg/s	-	-	-	252	The maximum circumferential temperature difference is observed as 16ºC (0.3 kg/s MFR) during the solar noon. However, at 2 h before solar noon, the maximum circumferential temperature difference for 0.3 kg/s MFR is 23.7ºC.
Nascimento, Zavaleta-aguilar, and Sim 2021[44]	Therminol ® 59, Therminol ® VP1, water and solar salt 40% KNO3 60% NaNO3	-	-	0.32 0.046 0.065 kg/s	-	273.4	69 70 55 71	300	Pressurized water had a greater performance as compared with Therminol vp-1 and solar salt, as it caused shorter absorber length up to 300ºC HTF outlet temperature.
Gharehdaghi et al. 2021[73]	SCO_2	-	-	0.839 kg/s	300	308.69 319.03 324.52 320.79 312.75	70.45 69.47 68.77 69.12 69.5	324.52	At 8 AM, thermal efficiency were 70.45%, at lowest DNI 740.43 W/m² and HTF inlet and outlet temperature difference is only 8.69 ºC. In contrast, at 12 PM, thermal efficiency were 68.77%, at maximum DNI 1286.21 W/m², and HTF inlet and outlet temperature difference is its peak about 24.52 ºC.

Malekpour, Ahmadi, and Sadeghzadeh 2021[46]	Thermal oil	-	-	0.067 kg/s	43.5	60 to 75	76	75	The employed PTSC produced warm water of 50 °C in middle of autumn, and 42 °C in the middle of winter. The heat transfer efficiency for these two times were 76% and 22.73%, respectively.
Nguimdo, Teka, and Fopossie 2021[47]	Water Therminol vp-1	-	-	0.6 kg/s	-	165 310 490	72.7	600	Pressurized steam at 40 bars was produced with a maximum temperature of 600 °C in direct mode and 490 °C in indirect mode for the month of February in Maroua with thermal efficiency of 72.7% in direct generation and 60.7% in indirect generation.
S. Mohammad, Hosseini, and Sha 2021[48]	Water	Al_2O_3 Graphene oxide (GO)	0.2	1,3,5	-	-	68.3	-	Nanofluids enhance the thermal efficiency compared to pure water that was observed at 1 L/min to be about 63.2% in GO nanofluid and 32.1% in Al_2O_3 nanofluid
Bellos, Tzivanidis, and Said 2020[49]	Syltherm 800	CU	0,2,4	25 to 300	100 200 300	-	-	350	Result show that nanofluid increases thermal efficiency and higher concentration of nanoparticle leads to higher thermal efficiency.
Fathabadi 2020[50]	H_2O	CUO	1	1 to 15	-	-	76.3	-	Obtained Thermal efficiency was 76.3% with PTC as compared to the evacuated tube solar collector (71.6%) and flat-plate solar collector FPC (74.9%).
Reddy and Ananthsornaraj 2020[51]	Therminol VP-1	-	-	0.12 kg/s	54.5	85	66	85	The results show that the average thermal efficiency for sunny and cloudy days is found to be 48.27% and 37.51% for both evacuated receiver and non evacuated receiver respectively.
Z. Zhao et al. 2020[52]	Air	-	-	Tube-0 76 116 126 Tube-1 72 112 121 Tube-2 71 117 129 Nm^3/h	38	293	Tube-1 39%	293	Solar irradiation and geometry of receiver tube significantly affects the air temperature gain. The higher temperature gain was shown by IPF-Tubes compared to than smooth tubes. The maximum air temperature rise was 266 °C and 166 °C for IPF-Tube #2 and S-Tube for air flow rate of 93Nm3/h in the similar DNI around 900 W/m^2.

Thappa et al. 2020[53]	-	-	-	100 to 300 LPH	-	127 to 327	-	-	System efficiency remarkably increased 79 to 81% in case-II study as compared to the reference system that was about 77 to 78% in case-I study.
Subramani, Sevvel, and Srinivasan 2020[54]	Distilled water(DI)	Al_2O_3	0.05	0.5 to 2	-	-	68	-	Water/Al_2O_3 nanofluid of 0.5% volume concentration with was studied at three flow rates (0.5, 1.0, 2.0 lpm). And absorber tube is coated with the carbon nano tubes. Results show that, the maximum collector efficiency of PTC enhanced by 8.6% in comparison with only water HTF.
Malan and K 2020[55]	Molten salt, NaK78, Liquid Sodium, Therminol VP1	-	-	0.897 0.9 0.876 0.929 0.905 kg/s	100.2 70.72 70.55 98.23 100.17	120.6 91.41 92.38 118.42 122.13	-	122.13	The least thermal gradient was obtained for liquid sodium that was, 17.81 K as compared with therminol VP1 i.e. 207.4 K, molten salt i.e. 175.29 K, and NaK78 i.e. 59.43 K, respectively.
Eduardo et al. 2020[56]	C2 Water C3 Thermal oil	-	-	-	C_2 76.52,92.22,93.04 C_3 114.38,125.21,111.92	-	47.8	-	The average useful energy gain of configuration C2 was approximately 22% higher than configuration C3 on the evaluated days. Thermal oil helped to reach higher temperatures by the proposed system, due to its lower volumetric heat capacity.
Xu et al. 2019[58]		-	-	40.35 m³/h	290	390	-	417.2	The optical efficiency is increased by 20%, the HTF outlet temperature is increased from 390 °C to 417.2 °C
Wang et al. 2019[59]	Syltherm 800	-	-	-	375.2 570.8 652.5 572 523.7 424 470.5	397 589.9 671 590.2 542.4 446.3 492.5	-	-	A MCRT-FVM-FEM simulation methods were used for analysis of SPTC system . The results between this and previous study show that they are in good agreement, which validate the method used is useful and credible.

Marefati, Mehrpooya, and Behshad 2018[62]	Water	Al_2O_3, CuO and Sic	1,3,5	0.03 kg/s	35,45,55	Tabriz- 225.3,226.71, 228.23 Tehran- 326.4,327.9,3 28.4 Yazd- 281.8,283.3,2 84.7 Shiraz- 254.1,255.9,2 57.9	19.01	328.4	Amongst the four locations, Shiraz was found most suitable location for SPTC system with annual efficiency of 13.91% and the highest monthly efficiency of 19.01% (June).
Tagle-Salazar, Nigam, and Rivera- Solorio 2018[64]	Water	Al_2O_3	0,1,3	7.53 gpm	56.3 54.1 54.8 56.4 59.1 63 57.6 39.2	57.2 55 55.7 57.2 59.9 63.8 58.5 40.3	60.596	63.8	-
Mwesigye, Yılmaz, and Meyer 2018[65]	Therminol ®VP-1	SWNCT (single wall carbon nano tubes) L-10 nm d-5 μm	0.25,0.5,1,2.5	1.63- 69.41 m^3/h	127-377	-	-	-	SWCNT thermal conductivity (2725 w/mk at 127°C and 1482 w/mk at 377°C). Thermal performance increase to 240% using SWCNT-Therminol VP-1 nano fluid at 2.5% volume fraction
Qu et al. 2017[66]	Dowtherm A	-	-	1.4-13.6 kg/s	195-214	262-305	67.4	305	With N-S tracking summer and winter daily average efficiency are 63% and 40% ,respectivly. With rotatable axis tracking winter daily average efficiency can be enhanced from 43% to 48%.
Sallaberry, Valenzuela, and Palacin 2017[67]	-	-	-	2.68-3.37 kg/s	170-340	-	66.2	-	-

Jamal-Abad, Saedodin, and Aminy 2017[68]	Water	-	-	0.5,1,1.5	-	-	-	-		Absorber filled with copper foam resulted in reduction about 45% overall loss coefficient U_L
Ebrahim Ghasemi and Akbar Ranjbar 2017[71]	Syltherm 800	-	-	-	-	-	-	-		Heat transfer behaviour of syltherm 800 HTF fluid carried out using numerical simulation. The porous rings used as turbulators inside absorber tube. Authors concluded that porous ring absorber with syltherm 800 HTF improved thermal performance as compared to smooth absorber tube.
Ameen et al. 2017[72]	H_2O	-	-	0.4,0.8,1.2	-	-	-	103		Results show that highest achievable temperature from 80 °C to 103 °C is in the duration of February to May of the year.

5. Receiver

Receiver converts the radiation in to heat and transfer the energy to the tube. Little heat losses with greater absorptance are key measures to select material for absorber. Expansion and contraction of the material during operation has the main problem with most of materials present today. To curtail the heat losses, special coating and thermal insulation is applied.

Many researchers are working on deflection in size of receiver and its effects on efficiency. Valdes, Almanza, and Soria (2014) summarized that the distortion or deflection occurs at very low flow rate of thermic fluid i.e. water[74]. Sandeep and Arunachala (2016) studied a viability of many augmentation techniques for heat transfer, such as application of tubular evacuated absorbers, nanofluid with and without inserts. Results shows that the use of turbulators with heat transfer fluid has been useful in laminar flow and turbulence flow. Nanofluids with turbulators are advantageous[75]. A MCRT method has been tested to determine the effects of a glass envelope on heat flux circulation on the absorber by Wang et al. (2015)[76]. Mostafa Esmaeili Shayan, Gholamhassan Najafi, Farzaneh Ghasemzadeh (2020) developed Aluminium (III) oxide glass to metal seal which also act as an insulator and found that system heat transfer efficiency improved by more than 30%[77].Khanna, Singh, and Kedare (2014) populated expression to check the distortion in the centroidal axis of the tube from the trough's focal line and concluded that the receiver tube stays un-distracted from the focal line at Rim angle[78].

Bortolato, Dugaria, and Del (2016) designed a new flat Al absorber as shown in Fig.5 with overall thermal efficiency of 64% in small parabolic trough collector and optical efficiency of around 82% at 0.160 km^2 W^{-1} with the little loss of pressure to count. The low MFR of thermic fluids in the receiver is required to generate steam that is the main advantage of the prototype [79]. Thermal performance, numerical simulation and mathematical models presented by Salgado Conrado, Rodriguez-Pulido, and Calderon (2017) for the experimental set up of Parabolic trough collector with an aim to understand the features of PTC for the researchers in future developments of PTC[80]. Prahl et al. (2017) compiled the root causes and effects for the displacement of receiver tube and also presented significant development in techniques to measure the displacement of the tube which is air borne measurement system[81].

Figure 5. Flat absorber developed by [79]

Gong et al. (2017), presented tubular receiver using pin fin arrangements placed in the PTC absorber tube and MCRT method along with FV (Finite Volume) Method considering to improve the overall heat transfer. During research they concluded 9% improvement in Nusselt number and 12% increase in overall heat transfer factor[82]. Potenza et al. (2017) has been used gas phase nanofluid as HTF in transparent absorber tube. They have used two concentric glass tube in which annulus space is being evacuated and inner glass tube is being used as absorber tube which is carrying Cuo nanoparticles dispersed in air as working medium. The average temperature of 145°C has been achieved for 10 h and maximum temperature of 180°C be reached with average thermal efficiency of 65%[83]. Jamal-Abad, Saedodin, and Aminy (2017) filled metal foam inside the absorber to improve the heat transfer of PTC along with improvement in performance. Reduction in efficiency with reduction of flux observed after inserting copper foam (Fig.6) having 0.9 porositiy and 30 PPI density[68].

Figure 6. Copper Foam [68]

The method is used to obtain the acceptance function of receiver with or without deviation, is only effective for normal position of reciever and with the variation[84]. Bitam et al. (2018) developed a mathematical approch to minimize thermal stress and losses of sinusoidal tube receiver and resulting in to higher performance of PTC system through lessening friction coefficient hike below 41%[85].

6. Sun Tracking system.

Sun tracking is classified as single axis and dual axis, as name implies, depend on number of tracking axes. Dual-axis tracking system tracks altitude-azimuth solar angles in order to keep incident radiation along the optical axis. Dual-axis mode can be further divided into the Polar axis-declination axis tracking mode and the elevation angle-azimuth tracking mode. Single-axis Sun tracking tracks either one of the elevation angle or azimuth, which can be accomplished by ensuring the incident light falls on the plane formed by the primary optical axis and the focal line. This type mainly includes the north-south tilt tracking mode, the north-south horizontal tracking mode and the east-west horizontal tracking mode[86].

Single axis tracking system has been recommended for optimum performance of any solar harvesting device. East-west alignment with no tracking is widely used for studies whereas; north-south alignment with east-west tracking is suitable for common applications[87]. Figure 7 and Figure 8 shows N-S alignments with E-W tracking and N-S tilt and E-W tracking modes respectively.
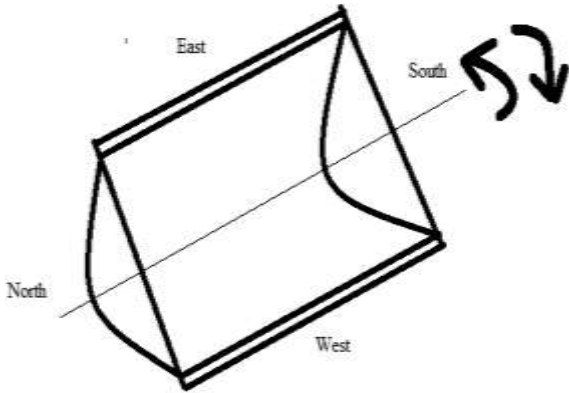

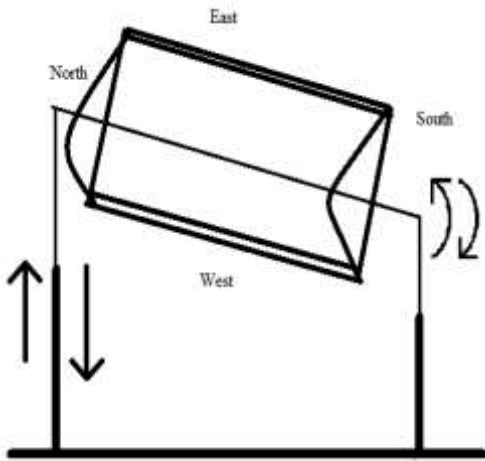**Figure 7.** North-south alignment with East-West tracking

Figure 8. North-South tilt with East-West tracking.

Qu et al. (2017) used rotatable axis tracking system in winter and improved overall collection efficiency by 5% when solar incidence angle is large. They also successfully lower the cosine loss by 10% in the same experimental model[66]. Gama et al. (2013) developed a portable receiver with single axis sun tracking system to diminish the optical losses by help of TRNSYS software[88].

Mageshwaran et al. (2018) improved less efficient helically coiled collector by incorporating a tracking system. Also experimented and reviewed another four tracking modes (an east–west alignment with one adjustment, an east–west alignment with continuous adjustment, north–south tracking horizontally with continuous adjustment, north–south axis which is parallel to the earth's axis with continuous adjustment) and concluded north-south axis rotation horizontally with the small and regular fine-tuning gives most optimum output than others[89]. Kumar and

Kumar (2018) came up with odd observation after testing non-evacuated tube with and without tracking system. And surprisingly they found non-tracking system has more output when used for small scale[90].
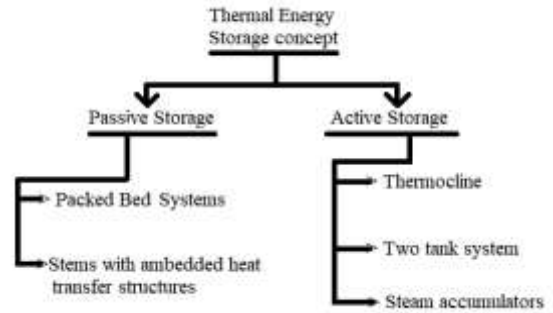
7. Thermal Storage Device

Figure 9. Classification of Thermal Storage Systems [87]

To store energy efficiently in the form of electricity or in the form of thermal is a challenging till date. Figure 9 categorised the thermal storage devices based on different ways. An exhaustive assessment on the evaluation of thermal storage devices for solar power plants has been done with design methodologies and factors at different levels, up to 500°C by Kuravi et al. 2013[91]. Kumaresan, Sridhar, and Velraj (2012) investigated the PTC with 230L storage capacity to check the performance. They concluded that shorter distance between PTC and storage device reduces the heat loss. Insulation of all components also helps the most, while the highest temperature is about 210°C in afternoon. The mass flow rate of 100 g/s and maximum temperature achieved was 116°C, the Fig.10 Shows photographic view of PTC designed by team[92].

Figure 10. Parabolic Trough Collector [92]

Jost et al. (2014) controlled the three-way valve that splits HTF between the steam generator and the storage system to run two systems simultaneously. To improve the performance-controlled inlet pressure were used to generate steam[93].

8. Discussion

The summary of the optical and thermal parameters is included in Table 2 and Table 3 respectively.

Following points are summarized

- Structure: Geometrical and Physical dimensions, cost and material selection, effect of wind force.
- Reflector: Cost and reflectivity of mirror, reflector coatings.
- Thermic fluids: Type of fluids, flow rate, maximum achievable temperature of HTF, effect of addition of nanoparticles
- Receiver: coatings, material and thermal conductivity, heat transfer augmentation technique-inserts
- Sun Tracking System: Position, N-S alignment/tilt and E-w tracking, Effect of tracking on optical efficiency
- Thermal energy storage: techniques- Active, passive

9. Research Gap

PTCs are most preferred options amongst the various concentrated solar power systems. Many researchers have studied the parabolic trough collector systems in reference to their design and performance evaluation in power generation, steam generation, process heat generation, etc. However, its application is limited to the dairy and food industry. Looking to their specific features, they can be utilized for meeting up the thermal energy requirements of various food and milk processing operations like pasteurization, sterilization, hot water generation systems, cleaning systems, etc. The economic cost analysis has to be carried out for capital investment, running cost and maintenance cost in order to asses payback period. Furthermore, more studies are required to evaluate manufacturing difficulties in smart designs and durability of PTC systems.

10. Conclusions

One of the most critical parameters for structure of PTC is its design, efficiency and initial cost. The improvement in design can leads to improvement in efficiency but sometimes leads to higher cost, which no doubt will be cover by improved efficiency. For storage devices or system, Heat Transfer Fluid is next important and essential component. HTF may be molten salt, thermic fluids to achieve temperature up to 600°C to generate steam resulted into generation of electricity in most cases. Design and selection of PTC plays major role in efficiency and application of system. New researches and developments are still under trial and are thriving to penetrate the market. This paper tries to covers realistic advancement and crucial points to be observe while designing, developing and / or even implementing the PTCS systems.

References

[1] S. Kyaligonza and E. Cetkin, "Photovoltaic System Efficiency Enhancement with Thermal Management: Phase Changing Materials (PCM) with High Conductivity Inserts," *Int. J. Smart grid*, vol. 5, no. 4, pp. 138–148, 2021, doi: 10.20508/ijsmartgrid.v5i4.218.g171.

[2] A. Harrouz and O. Harrouz, "Application of Solar Energies to Reinforce the Flow Water of Foggara in the Adrar Region," *Int. J. Smart grid*, vol. 2, no. 4, 2018, doi: 10.20508/ijsmartgrid.v2i4.32.g26.

[3] A. Alkholidi and H. Hamam, "Solar Energy Potentials in Southeastern European Countries: A Case Study," *Int. J. Smart grid*, vol. 3, no. 2, 2019, doi: 10.20508/ijsmartgrid.v3i2.51.g55.

[4] K. E. Okedu, H. A. L. Nadabi, and A. Aziz, "Prospects of Solar Energy in Oman: case of oil and gas industries," *Int. J. Smart grid*, vol. 3, no. 3, pp. 138–151, 2019, doi: 10.20508/ijsmartgrid.v3i3.68.g63.

[5] S. A. Kalogirou, *Solar thermal collectors and applications*, vol. 30, no. 3. 2004. doi: 10.1016/j.pecs.2004.02.001.

[6] S. K. Sahoo, "Renewable and sustainable energy reviews solar photovoltaic energy progress in India: A review," *Renew. Sustain. Energy Rev.*, vol. 59, pp. 927–939, 2016, doi: 10.1016/j.rser.2016.01.049.

[7] V. K. Jebasingh and G. M. J. Herbert, "A review of solar parabolic trough collector," *Renew. Sustain. Energy Rev.*, vol. 54, pp. 1085–1091, 2016, doi: 10.1016/j.rser.2015.10.043.

[8] I. Purohit and P. Purohit, "Performance assessment of grid-interactive solar photovoltaic projects under India's national solar mission," *Appl. Energy*, vol. 222, no. February, pp. 25–41, 2018, doi: 10.1016/j.apenergy.2018.03.135.

[9] A. Schweitzera, W. Schiela, M. Birklea, P. Navab, K.-J. Riffelmannb, A. Wohlfahrtc, G. Kuhlmannc, "ULTIMATE TROUGH® - Fabrication, erection and commissioning of the world's largest parabolic trough collector," *Energy Procedia*, vol. 49, pp. 1848–1857, 2014, doi: 10.1016/j.egypro.2014.03.196.

[10] I. E. P. Montesa, A. M. Beniteza, O. M. Chaveza, and A. E. L. Herrera, "Design and construction of a parabolic trough solar collector for process heat production," *Energy Procedia*, vol. 57, pp. 2149–2158, 2014, doi: 10.1016/j.egypro.2014.10.181.

[11] A. V. Arasu and T. Sornakumar, "Design , manufacture and testing of fiberglass reinforced parabola trough for parabolic trough solar collectors Indian Standard time," vol. 81, pp. 1273–1279, 2007, doi: 10.1016/j.solener.2007.01.005.

[12] O. Behar, A. Khellaf, and K. Mohammedi, "A novel parabolic trough solar collector model - Validation with experimental data and comparison to Engineering Equation Solver (EES)," *Energy Convers. Manag.*, vol. 106, pp. 268–281, 2015, doi: 10.1016/j.enconman.2015.09.045.

[13] B. Zou, J. Dong, Y. Yao, and Y. Jiang, "A detailed study on the optical performance of parabolic trough solar collectors with Monte Carlo Ray Tracing method based on theoretical analysis," *Sol. Energy*, vol. 147, pp. 189–201, 2017, doi: 10.1016/j.solener.2017.01.055.

[14] B. H. Upadhyay, "Parabolic Trough Collector, a Novel Design for Domestic Water Heating Application," *Int. J. Res. Appl. Sci. Eng. Technol.*, vol. V, no. X, pp. 497–503, 2017, doi:

10.22214/ijraset.2017.10073.

[15] J. Paetzold, S. Cochard, A. Vassallo, and D. F. Fletcher, "Wind engineering analysis of parabolic trough solar collectors: The effects of varying the trough depth," *J. Wind Eng. Ind. Aerodyn.*, vol. 135, pp. 118–128, 2014, doi: 10.1016/j.jweia.2014.10.017.

[16] B. Agagna, A. Smaili, Q. Falcoz, and O. Behar, "Experimental and numerical study of parabolic trough solar collector of MicroSol-R tests platform," *Exp. Therm. Fluid Sci.*, vol. 98, pp. 251–266, 2018, doi: 10.1016/j.expthermflusci.2018.06.001.

[17] A. Malan and K. Ravi Kumar, "A comprehensive review on optical analysis of parabolic trough solar collector," *Sustain. Energy Technol. Assessments*, vol. 46, no. November 2020, p. 101305, 2021, doi: 10.1016/j.seta.2021.101305.

[18] S. A. Kalogirou, "Chapter 3 - Solar Energy Collectors," *Sol. Energy Eng. (Second Ed.*, pp. 125–220, 2014, doi: 10.1016/B978-0-12-374501-9.00003-0.

[19] J. Macedo-Valencia, J. Ramírez-Ávila, R. Acosta, O. A. Jaramillo, and J. O. Aguilar, "Design, construction and evaluation of parabolic trough collector as demonstrative prototype," *Energy Procedia*, vol. 57, pp. 989–998, 2014, doi: 10.1016/j.egypro.2014.10.082.

[20] E. Bellos and C. Tzivanidis, "Alternative designs of parabolic trough solar collectors," *Progress in Energy and Combustion Science*, vol. 71. 2019. doi: 10.1016/j.pecs.2018.11.001.

[21] H. Hoseinzadeh, A. Kasaeian, M. Behshad, and M. Carlo, "Geometric optimization of parabolic trough solar collector based on the local concentration ratio using the Monte Carlo method," vol. 175, no. September, pp. 278–287, 2018, doi: 10.1016/j.enconman.2018.09.001.

[22] B. El Ghazzani, "Shape Optimization of A Parabolic Trough Collector, Geometrical Considerations," *Int. J. Eng. Res.*, vol. V10, no. 01, pp. 204–208, 2021, doi: 10.17577/ijertv10is010001.

[23] A. A. Shawky and A. K. H. Khalil, *Design and Performance Analysis of Small-Scale Parabolic Trough Solar Collectors Using Sustainable Materials*. Elsevier Ltd., 2018. doi: 10.1016/B978-0-12-803581-8.11136-1.

[24] A. Bharti and B. Paul, "Design of solar parabolic trough collector," *2017 Int. Conf. Adv. Mech. Ind. Autom. Manag. Syst. AMIAMS 2017 - Proc.*, no. February, pp. 302–306, 2017, doi: 10.1109/AMIAMS.2017.8069229.

[25] J. a. Duffie, W. a. Beckman, and W. M. Worek, *Solar Engineering of Thermal Processes, 4nd ed.*, vol. 116. 2003. doi: 10.1115/1.2930068.

[26] K. Lovegrove and J. Pye, "Fundamental principles of concentrating solar power (CSP) systems," *Conc. Sol. Power Technol.*, pp. 16–67, 2012, doi: 10.1533/9780857096173.1.16.

[27] M. Günther, M. Joemann, and S. Csambor, "Advanced CSP Teaching Materials Chapter 5 Parabolic Trough Technology Authors," *2011*, pp. 1–

43, 2011.

[28] A. A. Sagade, S. Aher, and N. N. Shinde, "Performance evaluation of low-cost FRP parabolic trough reflector with mild steel receiver," vol. 93, no. 1986, pp. 1–8, 2013.

[29] A. A. Sagade, P. N. N. Shinde, and P. P. S. Patil, "Effect of receiver temperature on performance evaluation of silver coated selective surface compound parabolic reflector with top glass cover," *Energy Procedia*, vol. 48, pp. 212–222, 2014, doi: 10.1016/j.egypro.2014.02.026.

[30] J. E. Pacheco, S. N. Laboratories, T. Wolf, and N. Muley, "Incorporating Supercritical Steam Turbines into Advanced Molten-Salt Power Tower Plants : Feasibility and Performance," no. September 2014, 2013, doi: 10.13140/2.1.3873.2167.

[31] E. Bellos and C. Tzivanidis, "Thermal efficiency enhancement of nanofluid-based parabolic trough collectors," *J. Therm. Anal. Calorim.*, vol. 135, no. 1, pp. 597–608, 2019, doi: 10.1007/s10973-018-7056-7.

[32] A. K. Hussein, "Applications of nanotechnology to improve the performance of solar collectors - Recent advances and overview," *Renew. Sustain. Energy Rev.*, vol. 62, pp. 767–792, 2016, doi: 10.1016/j.rser.2016.04.050.

[33] F. Zaversky, R. Medina, J. García-Barberena, M. Sánchez, and D. Astrain, "Object-oriented modeling for the transient performance simulation of parabolic trough collectors using molten salt as heat transfer fluid," *Sol. Energy*, vol. 95, pp. 192–215, 2013, doi: 10.1016/j.solener.2013.05.015.

[34] S. E. Ghasemi and A. A. Ranjbar, "Thermal performance analysis of solar parabolic trough collector using nanofluid as working fluid: A CFD modelling study," *J. Mol. Liq.*, vol. 222, pp. 159–166, 2016, doi: 10.1016/j.molliq.2016.06.091.

[35] E. Bellos, C. Tzivanidis, and K. A. Antonopoulos, "A detailed working fluid investigation for solar parabolic trough collectors," *Appl. Therm. Eng.*, vol. 114, pp. 374–386, 2017, doi: 10.1016/j.applthermaleng.2016.11.201.

[36] R. P. Praveen and K. V. V Chandra, "Performance enhancement of parabolic trough collector solar thermal power plants with thermal energy storage capability System Advisor model," *Ain Shams Eng. J.*, vol. 13, no. 5, p. 101716, 2022, doi: 10.1016/j.asej.2022.101716.

[37] K. Zhao, H. Jin, Z. Gai, and H. Hong, "A thermal efficiency-enhancing strategy of parabolic trough collector systems by cascadingly applying multiple solar selective-absorbing coatings," *Appl. Energy*, vol. 309, no. December 2021, p. 118508, 2022, doi: 10.1016/j.apenergy.2021.118508.

[38] M. Ghodbane, B. Boumeddane, A. Khechekhouche, and S. Largot, "Materials Today : Proceedings Study of the effect of the position and metal of the receiver tube on the performance of a parabolic trough solar collector," *Mater. Today Proc.*, no. xxxx, 2022, doi: 10.1016/j.matpr.2021.12.497.

[39] B. Shaker, M. Gholinia, M. Pourfallah, and D. D.

Ganji, "Highlights for Review," *Theor. Appl. Mech. Lett.*, p. 100323, 2022, doi: 10.1016/j.taml.2022.100323.

[40] K. Mohammadi, S. Khanmohammadi, J. Immonen, and K. Powell, "Techno-economic analysis and environmental benefits of solar industrial process heating based on parabolic trough collectors," *Sustain. Energy Technol. Assessments*, vol. 47, no. May, p. 101412, 2021, doi: 10.1016/j.seta.2021.101412.

[41] M. Khan, I. N. Alsaduni, M. Alluhaidan, W. Xia, and M. Ibrahim, "Evaluating the energy ef fi ciency of a parabolic trough solar collector fi lled with a hybrid nano fl uid by utilizing double fl uid system and a novel corrugated absorber tube," vol. 000, pp. 1–12, 2021, doi: 10.1016/j.jtice.2021.04.045.

[42] A. M. Norouzi, M. Siavashi, R. Ahmadi, and M. Tahmasbi, "Experimental study of a parabolic trough solar collector with rotating absorber tube," *Renew. Energy*, vol. 168, pp. 734–749, 2021, doi: 10.1016/j.renene.2020.12.088.

[43] R. K. Pal and R. K. K, "Two- fl uid modeling of direct steam generation in the receiver of parabolic trough solar collector with non-uniform heat fl ux," *Energy*, vol. 226, p. 120308, 2021, doi: 10.1016/j.energy.2021.120308.

[44] F. I. Nascimento, E. W. Zavaleta-Aguilar, and J. R. Simões-Moreira, "Algorithm for sizing parabolic-trough solar collectors," *Therm. Sci. Eng. Prog.*, vol. 24, no. December 2020, 2021, doi: 10.1016/j.tsep.2021.100932.

[45] A. A. Alnaqi, J. Alsarraf, and A. A. A. Al-rashed, "Hydrothermal effects of using two twisted tape inserts in a parabolic trough solar collector filled with MgO-MWCNT / thermal oil hybrid nanofluid," *Sustain. Energy Technol. Assessments*, vol. 47, no. March, p. 101331, 2021, doi: 10.1016/j.seta.2021.101331.

[46] A. Malekpour, R. Ahmadi, and S. Sadeghzadeh, "In situ latent thermal energy storage in underfloor heating system of building connected to the parabolic trough solar collector-an experimental study," *J. Energy Storage*, vol. 44, no. PB, p. 103489, 2021, doi: 10.1016/j.est.2021.103489.

[47] L. A. Nguimdo, J. Teka, and F. D. Fopossie, "Thermal Analysis of Parabolic Trough Solar Collector and Assessment of Steam Power Potential at Two Locations in Cameroon," vol. 11, no. 3, 2021.

[48] S. Mohammad, S. Hosseini, and M. Sha, "An experimental study on energetic performance evaluation of a parabolic trough solar collector operating with Al 2 O 3 / water and GO / water nano fl uids," vol. 234, 2021, doi: 10.1016/j.energy.2021.121317.

[49] E. Bellos, C. Tzivanidis, and Z. Said, "Original article A systematic parametric thermal analysis of nano fl uid-based parabolic trough solar collectors," *Sustain. Energy Technol. Assessments*, vol. 39, no. March, p. 100714, 2020, doi: 10.1016/j.seta.2020.100714.

[50] H. Fathabadi, "Novel low-cost parabolic trough solar collector with TPCT heat pipe and solar tracker : Performance and comparing with commercial fl at-plate and evacuated tube solar collectors," *Sol. Energy*, vol. 195, no. November 2019, pp. 210–222, 2020, doi: 10.1016/j.solener.2019.11.057.

[51] K. S. Reddy and C. Ananthsornaraj, "Design , development and performance investigation of solar Parabolic Trough Collector for large-scale solar power plants," *Renew. Energy*, vol. 146, pp. 1943–1957, 2020, doi: 10.1016/j.renene.2019.07.158.

[52] Z. Zhao, F. Bai, X. Zhang, and Z. Wang, "Experimental study of pin finned receiver tubes for a parabolic trough solar air collector," *Sol. Energy*, vol. 207, no. 6, pp. 91–102, 2020, doi: 10.1016/j.solener.2020.06.070.

[53] S. Thappa, A. Chauhan, Y. Anand, and S. Anand, "Materials Today : Proceedings Analytical comparison of two distinct receiver tubes of a parabolic trough solar collector system for thermal application," *Mater. Today Proc.*, no. xxxx, pp. 2–7, 2020, doi: 10.1016/j.matpr.2020.04.257.

[54] J. Subramani, P. Sevvel, Anbuselvam, and S. A. Srinivasan, "Influence of CNT coating on the efficiency of solar parabolic trough collector using AL2O3 nanofluids - A multiple regression approach," *Mater. Today Proc.*, vol. 45, no. xxxx, pp. 1857–1861, 2021, doi: 10.1016/j.matpr.2020.09.047.

[55] A. Malan and K. Ravi Kumar, "Coupled optical and thermal analysis of large aperture parabolic trough solar collector," *Int. J. Energy Res.*, vol. 45, no. 3, pp. 4630–4651, 2021, doi: 10.1002/er.6128.

[56] M. Eduardo, V. De Araujo, S. Renato, E. G. Pereira, and M. D. O. Resende, "Experimental evaluation of a stationary parabolic trough solar collector : In fl uence of the concentrator and heat transfer fl uid," vol. 276, 2020, doi: 10.1016/j.jclepro.2020.124174.

[57] A. J. Abdulhamed, M. H. Rasheed, H. K. Kareem, N. Mariah, M. Z. A. Ab-kadir, and A. A. Hairuddin, "Design and Performance Testing of a Parabolic Trough Collector Including Deformation Test of the Receiver Tube," vol. 2, no. 2, pp. 47–65, 2020.

[58] Li Xu, Feihu Sun, Linrui Ma, Xiaolei Li, Dongqiang Lei, Guofeng Yuan, Huibin Zhu, Qiangqiang Zhang, Ershu Xu, Zhifeng Wang, "Analysis of optical and thermal factors' effects on the transient performance of parabolic trough solar collectors," *Sol. Energy*, vol. 179, no. June 2018, pp. 195–209, 2019, doi: 10.1016/j.solener.2018.12.070.

[59] X. Wang, S. Luo, T. Tang, X. Liu, and Y. He, "A MCRT-FVM-FEM coupled simulation for optical-thermal-structural analysis of parabolic trough solar collectors," *Energy Procedia*, vol. 158, pp. 477–482, 2019, doi: 10.1016/j.egypro.2019.01.138.

[60] M. A. Ehyaei, A. Ahmadi, M. El Haj Assad, and T. Salameh, "Optimization of parabolic through collector (PTC) with multi objective swarm optimization (MOPSO) and energy, exergy and economic analyses," *J. Clean. Prod.*, vol. 234, pp. 285–296, 2019, doi: 10.1016/j.jclepro.2019.06.210.

[61] M. El Ydrissi, H. Ghennioui, E. G. Bennouna, and A.

1586

Farid, "Geometric, optical and thermal analysis for solar parabolic trough concentrator efficiency improvement using the photogrammetry technique under semi-arid climate," *Energy Procedia*, vol. 157, no. February, pp. 1050–1060, 2019, doi: 10.1016/j.egypro.2018.11.272.

[62] M. Marefati, M. Mehrpooya, and M. B. Shafii, "Optical and thermal analysis of a parabolic trough solar collector for production of thermal energy in different climates in Iran with comparison between the conventional nanofluids," *J. Clean. Prod.*, vol. 175, pp. 294–313, 2018, doi: 10.1016/j.jclepro.2017.12.080.

[63] H. Hoseinzadeh, A. Kasaeian, and M. Behshad Shafii, "Geometric optimization of parabolic trough solar collector based on the local concentration ratio using the Monte Carlo method," *Energy Convers. Manag.*, vol. 175, no. April, pp. 278–287, 2018, doi: 10.1016/j.enconman.2018.09.001.

[64] P. D. Tagle-Salazar, K. D. P. Nigam, and C. I. Rivera-Solorio, "Heat transfer model for thermal performance analysis of parabolic trough solar collectors using nanofluids," *Renew. Energy*, vol. 125, pp. 334–343, 2018, doi: 10.1016/j.renene.2018.02.069.

[65] A. Mwesigye, İ. H. Yılmaz, and J. P. Meyer, "Numerical analysis of the thermal and thermodynamic performance of a parabolic trough solar collector using SWCNTs-Therminol®VP-1 nanofluid," *Renew. Energy*, vol. 119, pp. 844–862, 2018, doi: 10.1016/j.renene.2017.10.047.

[66] W. Qu, R. Wang, H. Hong, J. Sun, and H. Jin, "Test of a solar parabolic trough collector with rotatable axis tracking," *Appl. Energy*, vol. 207, pp. 7–17, 2017, doi: 10.1016/j.apenergy.2017.05.114.

[67] F. Sallaberry, L. Valenzuela, and L. G. Palacin, "On-site parabolic-trough collector testing in solar thermal power plants: Experimental validation of a new approach developed for the IEC 62862-3-2 standard," *Sol. Energy*, vol. 155, pp. 398–409, 2017, doi: 10.1016/j.solener.2017.06.045.

[68] M. T. Jamal-Abad, S. Saedodin, and M. Aminy, "Experimental investigation on a solar parabolic trough collector for absorber tube filled with porous media," *Renew. Energy*, vol. 107, pp. 156–163, 2017, doi: 10.1016/j.renene.2017.02.004.

[69] A. Houcine, T. Maatallah, S. El Alimi, and S. Ben Nasrallah, "Optical modeling and investigation of sun tracking parabolic trough solar collector basing on Ray Tracing 3Dimensions-4Rays," *Sustain. Cities Soc.*, vol. 35, no. October 2016, pp. 786–798, 2017, doi: 10.1016/j.scs.2017.08.031.

[70] B. Zou, H. Yang, Y. Yao, and Y. Jiang, "A detailed study on the effects of sunshape and incident angle on the optical performance of parabolic trough solar collectors," *Appl. Therm. Eng.*, vol. 126, pp. 81–91, 2017, doi: 10.1016/j.applthermaleng.2017.07.149.

[71] S. Ebrahim Ghasemi and A. Akbar Ranjbar, "Numerical thermal study on effect of porous rings on performance of solar parabolic trough collector," *Appl. Therm. Eng.*, vol. 118, pp. 807–816, 2017, doi:

10.1016/j.applthermaleng.2017.03.021.

[72] S. Ameen, H. V Byregowda, M. Mohsin, H. Ali, and M. Imran, "Resource-Efficient Technologies Experimental and simulation studies of parabolic trough collector design for obtaining solar energy," *Resour. Technol.*, vol. 3, no. 4, pp. 414–421, 2017, doi: 10.1016/j.reffit.2017.03.003.

[73] S. Gharehdaghi, S. F. Moujaes, and A. Mahdavi Nejad, "Thermal-fluid analysis of a parabolic trough solar collector of a direct supercritical carbon dioxide Brayton cycle: A numerical study," *Sol. Energy*, vol. 220, no. February, pp. 766–787, 2021, doi: 10.1016/j.solener.2021.03.039.

[74] A. Valdés, R. Almanza, and A. Soria, "Determining the deflection magnitude of a steel receiver from a DSG parabolic trough concentrator under stratified flow conditions," *Energy Procedia*, vol. 57, pp. 341–350, 2014, doi: 10.1016/j.egypro.2014.10.039.

[75] H. M. Sandeep and U. C. Arunachala, "Solar parabolic trough collectors: A review on heat transfer augmentation techniques," *Renew. Sustain. Energy Rev.*, vol. 69, no. August 2015, pp. 1218–1231, 2017, doi: 10.1016/j.rser.2016.11.242.

[76] F. Wang, J. Tan, L. Ma, and C. Wang, "Effects of glass cover on heat flux distribution for tube receiver with parabolic trough collector system," *Energy Convers. Manag.*, vol. 90, pp. 47–52, 2015, doi: 10.1016/j.enconman.2014.11.004.

[77] M. E. Shayan, G. Najafi, and F. Ghasemzadeh, "Advanced Study of the Parabolic Trough Collector Using Aluminum (III) Oxide," vol. 4, no. 3, 2020.

[78] S. Khanna, S. Singh, and S. B. Kedare, "Effect of angle of incidence of sun rays on the bending of absorber tube of solar parabolic trough concentrator," *Energy Procedia*, vol. 48, no. December, pp. 123–129, 2014, doi: 10.1016/j.egypro.2014.02.015.

[79] M. Bortolato, S. Dugaria, and D. Del Col, "Experimental study of a parabolic trough solar collector with flat bar-and-plate absorber during direct steam generation," *Energy*, vol. 116, pp. 1039–1050, 2016, doi: 10.1016/j.energy.2016.10.021.

[80] L. Salgado Conrado, A. Rodriguez-Pulido, and G. Calderón, "Thermal performance of parabolic trough solar collectors," *Renew. Sustain. Energy Rev.*, vol. 67, pp. 1345–1359, 2017, doi: 10.1016/j.rser.2016.09.071.

[81] C. Prahl, M. Röger, B. Stanicki, and C. Hilgert, "Absorber tube displacement in parabolic trough collectors – A review and presentation of an airborne measurement approach," *Sol. Energy*, vol. 157, pp. 692–706, 2017, doi: 10.1016/j.solener.2017.05.023.

[82] X. Gong, F. Wang, H. Wang, J. Tan, Q. Lai, and H. Han, "Heat transfer enhancement analysis of tube receiver for parabolic trough solar collector with pin fin arrays inserting," *Sol. Energy*, vol. 144, pp. 185–202, 2017, doi: 10.1016/j.solener.2017.01.020.

[83] M. Potenza, M. Milanese, G. Colangelo, and A. de Risi, "Experimental investigation of transparent parabolic trough collector based on gas-phase nanofluid," *Appl. Energy*, vol. 203, pp. 560–570,

2017, doi:
https://doi.org/10.1016/j.apenergy.2017.06.075.

[84]   N. Fraidenraich, M. Henrique, D. O. P. Filho, and O. De, "A new approach for obtaining angular acceptance function of non-perfect parabolic concentrating collectors," *Sol. Energy*, vol. 147, pp. 455–462, 2017, doi: 10.1016/j.solener.2017.03.052.

[85]   E. W. Bitam, Y. Demagh, A. A. Hachicha, H. Benmoussa, and Y. Kabar, "Numerical investigation of a novel sinusoidal tube receiver for parabolic trough technology," *Appl. Energy*, vol. 218, no. February, pp. 494–510, 2018, doi: 10.1016/j.apenergy.2018.02.177.

[86]   L. Kong, Y. Zhang, Z. Lin, Z. Qiu, C. Li, and P. Le, "Optimal design of the solar tracking system of parabolic trough concentrating collectors," *Int. J. Low-Carbon Technol.*, vol. 15, no. 4, pp. 613–619, 2020, doi: 10.1093/ijlct/ctaa065.

[87]   B. H. Upadhyay, A. J. Patel, and P. V. Ramana, "A detailed review on solar parabolic trough collector," *Int. J. Ambient Energy*, vol. 0750, pp. 1–21, 2019, doi: 10.1080/01430750.2019.1636869.

[88]   A. Gama, C. Larbes, A. Malek, F. Yettou, and B. Adouane, "Design and realization of a novel sun tracking system with absorber displacement for parabolic trough collectors," *J. Renew. Sustain. Energy*, vol. 5, no. 3, 2013, doi: 10.1063/1.4807476.

[89]   G. Mageshwaran, S. Ramachandran, K. Gobinath, and R. B. Durairaj, "Design of tracking system for helical-coiled receiver tube of parabolic trough collector," *Int. J. Ambient Energy*, vol. 0, no. 0, pp. 1–5, 2017, doi: 10.1080/01430750.2016.1230782.

[90]   D. Kumar and S. Kumar, "Thermal performance of the solar parabolic trough collector at different flow rates: an experimental study," *Int. J. Ambient Energy*, vol. 39, no. 1, pp. 93–102, 2018, doi: 10.1080/01430750.2016.1269673.

[91]   S. Kuravi, J. Trahan, D. Y. Goswami, M. M. Rahman, and E. K. Stefanakos, "Thermal energy storage technologies and systems for concentrating solar power plants," *Prog. Energy Combust. Sci.*, vol. 39, no. 4, pp. 285–319, 2013, doi: 10.1016/j.pecs.2013.02.001.

[92]   G. Kumaresan, R. Sridhar, and R. Velraj, "Performance studies of a solar parabolic trough collector with a thermal energy storage system," *Energy*, vol. 47, no. 1, pp. 395–402, 2012, doi: 10.1016/j.energy.2012.09.036.

[93]   M. Jost, W. Grote, F. Möllenbruck, and M. Mönnigmann, "Plant-wide control of a parabolic trough power plant with thermal energy storage," *IFAC Proc. Vol.*, vol. 19, pp. 419–425, 2014, doi: 10.3182/20140824-6-za-1003.00879.